

**Table II.** Observed and Calculated Second Moments ( $G^2$ )

Structure	$M_{2\text{intra}}$	$M_{2\text{inter}}$	$M_{2\text{calcd}}$	$M_{2\text{obsd}}$
Rigid	36.1	4	$40.1 \pm 2$	
Me rot.	14.1	2.5	$16.6 \pm 2$	17.4
N inv.	12.4	2	$14.4 \pm 2$	
Flex	8.1	2	$10.1 \pm 2$	10.7
Flex + N inv	7.8	1.7	$9.5 \pm 2$	10.7

treatment), which is not consistent with the experimental observation. These results are summarized in Table II.

**Acknowledgments.** We wish to thank Dr. H. K. Yuen of the Monsanto Corporation for running the differential scanning calorimeter study and Mr. W. F. Paton for calculation of the interproton distances used for the second moment. J.Y.C. acknowledges the support of NIH Research Grant No. R01NS10903 from National Institute of Neurological Diseases and Stroke. We also wish to thank Dr. E. R. Corey for helpful discussions and the McDonnell Douglas Astronautics Co. for the use of a storage oscilloscope.

## References and Notes

- (1) For a review of this technique, see L. M. Jackman and F. A. Cotton, Ed., "Dynamic Nuclear Magnetic Resonance Spectroscopy", Academic Press, New York, N.Y., 1975. There are other NMR techniques that have been used in some cases to study these processes, such as spin echo, relaxation in the rotating frame, wiggle decay, and saturation transfer.
- (2) W. F. Paton, J. P. Paton, J. Y. Corey, and E. R. Corey, Abstracts, 170th National Meeting of the American Chemical Society, Chicago, Ill., Aug. 1975, No. INOR-61.
- (3) A. D. Hardy and F. R. Ahmed, *Acta Crystallogr., Sect. B*, **30**, 1674 (1974).
- (4) A. D. Hardy and F. R. Ahmed, *Acta Crystallogr., Sect. B*, **30**, 1670 (1974).
- (5) R. R. Fraser, M. H. Raza, R. N. Renaud, and R. B. Layton, *Can. J. Chem.*, **53**, 167 (1975).
- (6) T. C. Farrar and E. D. Becker, "Pulse and Fourier Transform NMR", Academic Press, New York, N.Y., 1971.
- (7) J. Jeener and P. Broekaert, *Phys. Rev.*, **157**, 232 (1967).
- (8) A. Abragam, "The Principles of Nuclear Magnetism", Clarendon Press, Oxford, England, 1961, p 106.
- (9) J. G. Powles and J. H. Strange, *Proc. Phys. Soc., London*, **82**, 6 (1963).
- (10) P. Mansfield, *Phys. Rev.*, **137**, A961 (1965).
- (11) N. Bloembergen, E. M. Purcell, and R. V. Pound, *Phys. Rev.*, **73**, 679 (1948).
- (12) G. P. Jones, *Phys. Rev.*, **148**, 332 (1966).
- (13) D. C. Aillon, *Adv. Magn. Reson.*, **5**, 177 (1971).
- (14) D. C. Aillon and C. P. Slichter, *Phys. Rev.*, **135**, 1099 (1964); **137**, 235 (1965).
- (15) O. Lauer, D. Stehlik, and K. H. Hausser, *J. Magn. Reson.*, **6**, 524 (1972).
- (16) H. S. Gutowsky and G. E. Pake, *J. Chem. Phys.*, **18**, 162 (1950).
- (17) E. R. Andrew and G. J. Jenks, *Proc. Phys. Soc.*, **80**, 663 (1962).
- (18) The position of the  $T_{1\rho}$  minimum depends upon the strength of the rf field  $H_1$  (see eq 12).
- (19) The position of the  $T_1$  minimum depends upon the strength of the strong field  $H_1$  (see eq 12).
- (20) L. C. Hebel, *Solid State Phys.*, **15**, 409 (1963).
- (21) D. C. Douglass and G. P. Jones, *J. Chem. Phys.*, **45**, 956 (1966).
- (22) It should be noted that this range is expected to be even larger in favorable cases.
- (23) H. K. Yuen, unpublished results.
- (24) R. Van Steenwinkel, *Z. Naturforsch., A*, **24**, 1526 (1969).
- (25) J. H. Van Vleck, *Phys. Rev.*, **74**, 1168 (1948).
- (26) G. W. Smith, *J. Chem. Phys.*, **42**, 4229 (1965).
- (27) J. G. Powles and H. S. Gutowsky, *J. Chem. Phys.*, **21**, 1704 (1953).
- (28) D. W. Larsen and T. A. Smentkowski, results to be published.
- (29) J. M. Chezeau, J. Dufourcq, and J. H. Strange, *Mol. Phys.*, **20**, 305 (1971).
- (30) E. A. Andrew and R. G. Eades, *Proc. Phys. Soc., London, Sect. A*, **216**, 398 (1953).
- (31) J. M. Lehn and J. Wagner, *J. Chem. Soc. D*, 414 (1970); *Tetrahedron*, **26**, 4227 (1970).
- (32) A. T. Bottini and J. D. Roberts, *J. Am. Chem. Soc.*, **80**, 5203 (1958).
- (33) J. Stackhouse, R. D. Baechler, and K. Mislow, *Tetrahedron Lett.*, 3437 (1971).
- (34) I. J. Ferguson, A. R. Katritzky, and D. M. Read, *Chem. Commun.*, 255 (1975).
- (35) F. A. L. Anet, I. Yarari, I. J. Ferguson, A. R. Katritzky, M. Moreno-Manas, and M. J. T. Robinson, *Chem. Commun.*, 399 (1976).
- (36) See, for example: M. Polak and M. Sheinblatt, *J. Magn. Reson.*, **12**, 261 (1973), in which an activation barrier  $>6$  kcal/mol for methyl reorientation is reported.

## Nuclear Magnetic Resonance in Pulse Radiolysis. 2. CIDNP in Radiolysis of Aqueous Solutions<sup>1,2</sup>

A. D. Trifunac\* and D. J. Nelson<sup>3</sup>

*Contribution from the Chemistry Division, Argonne National Laboratory, Argonne, Illinois 60439. Received August 10, 1976*

**Abstract:** Applications of magnetic resonance to the study of radiolysis are illustrated. The products of radiolytically produced radicals exhibit CIDNP when examined, seconds after their creation, by NMR. Irradiation with a pulsed electron beam (3 MeV) was carried out in variable magnetic fields and the irradiated solutions were transferred to the NMR sample tube using a fast flow system. Aqueous solutions of methanol, iodomethane, ethylene glycol, acetate, and chloroacetate were studied. In these systems CIDNP in numerous products and starting materials can be observed. The "primary radicals" of radiolysis  $e_{\text{aq}}^-$  and H play a significant role in the polarization pathways. Applicability of the radical pair model of CIDNP to radiation chemistry is illustrated.

In radiolysis when dilute aqueous solutions are irradiated practically all the energy absorbed is deposited in water molecules and the observed chemical changes are brought about indirectly via the radical products.<sup>4</sup> The primary radicals produced in water radiolysis are OH,  $e_{\text{aq}}^-$ , and H. These radicals react with themselves and with solutes dissolved in water. In this work we will be primarily concerned with radicals produced by OH abstraction from organic alcohols and acids and by the  $e_{\text{aq}}^-$  dissociative electron capture in alkyl halides. Both primary and secondary radicals in pulse radiolysis have

been studied using several methods; the fast optical detection and electron paramagnetic resonance (EPR) are two such techniques.<sup>4</sup>

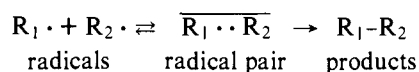
For some time now, we have been interested in applications of magnetic resonance to the study of pulse radiolysis, especially in the various manifestations of the chemically induced magnetic polarization phenomena. The observation of non-equilibrium electron spin populations in radicals, the so-called chemically induced dynamic electron polarization (CIDEP), in the microsecond domain<sup>5,6</sup> and the observation of the re-

sidual spin population from the radical precursors in the sub-microsecond domain<sup>7</sup> can substantially add to the understanding of the radical reaction mechanisms.

Most recently we have applied nuclear magnetic resonance spectroscopy to the study of chemically induced dynamic nuclear polarization (CIDNP) in products of radiolytically generated radicals.<sup>2</sup> If the products are examined by NMR within several seconds after their formation, nonequilibrium population of nuclear spins CIDNP can be observed. The study of CIDEP and CIDNP provides details of radical-radical interaction in solution.<sup>8</sup> CIDNP in the radical reaction products and CIDEP in the radicals reflect the memory of previous radical encounters. The time domain of and the information provided by these two magnetic polarization phenomena are complementary.

Our primary intent is to show how the qualitative examination of CIDNP in products of radiolysis in varying magnetic fields and under different reaction conditions provides new mechanistic details of the radiolytic reactions. We first present a brief outline of CIDNP as it applies to products in pulse radiolysis.

In radiolysis, two independently generated radicals can give rise to a radical pair, which consists of two weakly interacting doublet states:



The components of such a radical pair can combine and/or disproportionate to give a diamagnetic product or can diffuse apart to give free radicals. There is a finite probability that radicals which have encountered each other in a radical pair and have subsequently diffused apart might encounter again. Polarization is developed during these diffusive excursions of the radical pair components. This polarization results from singlet-triplet mixing of the electron-nuclear states of the radical pair manifold. The spin Hamiltonian is field dependent, and as a consequence both relative and absolute intensities of CIDNP spectra are a function of the magnetic field. In high magnetic fields (>1000 G) the mixing of the two nearest states of the singlet-triplet manifold of the radical pair (S-T<sub>0</sub>) is usually dominant. At lower magnetic fields (>1000 G) S-T<sub>±1</sub> transitions become important.

In the radical pair spin Hamiltonian matrix the off-diagonal elements connecting T<sub>0</sub> and S show that these states are mixed by the difference in the sums of the hyperfine interactions on the two components of the radical pair. These same elements connect only states whose nuclear spin functions are identical. In practice CIDNP NMR spectra in the high-field region are dominated by *g*-factor differences of the two components of the radical pair.

The high-field CIDNP effects can be classified into what are known as the "multiplet effect" and the "net effect". The multiplet effect is the observation of both enhanced absorption (A) and emission (E) in the multiplet of lines originating from transitions of groups of identical nuclei coupled to other nuclei by indirect nuclear spin coupling. The net effect is manifested when a line or group of lines, belonging to a single group of nuclei, exhibit either enhanced absorption or emission. The net effect is observed when radical pair components have different *g* factors.<sup>9</sup> If the two components of the radical pair have identical *g* factors only a pure multiplet effect is observed. The observation of the multiplet effect requires at least two different coupled nuclei; thus, for a single group of nuclei (that are not coupled), only the net effect contributes to CIDNP. Frequently the combination of the two effects is observed. That is, the superposition of the net effect on the multiplet effect yields polarized NMR multiplets that show an AE multiplet effect with excess E or A. Two simple algorithms have been

described which enable prediction of phase of high-field CIDNP spectra.<sup>10</sup>

At low fields the size of the singlet-triplet energy difference (exchange coupling, *J*), the Zeeman splittings, and the hyperfine coupling become similar; thus, S-T<sub>±1</sub> processes may also contribute to CIDNP. Off-diagonal elements of the radical pair spin Hamiltonian connecting S with T<sub>±1</sub> involve the hyperfine interactions only and are associated with a change in the nuclear spin. Specifically, if the singlet state is below the triplet state (*J* < 0), the S-T<sub>-1</sub> process can predominate and the spectrum will appear in emission. (The converse also holds.) Even if the exchange coupling (*J*) is zero,<sup>11</sup> polarization can arise from unequal S-T<sub>±1</sub> transitions when the magnetic field approaches the magnitude of the hyperfine coupling. As a result negative hyperfine coupling gives emission and positive hyperfine coupling gives enhanced absorption. In all cases that we have examined in radiolysis we observe emission at low fields.

At zero field CIDNP of a single nucleus or group of nuclei vanishes because a preferred axis of quantization does not exist. However, zero-field CIDNP can be observed for systems in which nuclear spins are coupled by indirect nuclear coupling in the products as a consequence of unequal zero-field energy-level populations.

The noticeable feature of zero-field CIDNP is the absence of the inner lines of the multiplets of the A<sub>*m*</sub>X<sub>*n*</sub> nuclear spin system. While in this work we report no true zero-field CIDNP spectra, at our lowest field used (~30 G) the inner lines of several multiplets were observed to be noticeably weaker.

To supplement this brief outline of CIDNP the reader is referred to an excellent discussion of CIDNP in a review by Closs.<sup>12</sup>

## Experimental Section

**Reagents.** All chemicals used in this study were of the highest purity available and were used without further purification. Solutions were prepared in deuterium oxide and were degassed by bubbling He or N<sub>2</sub>O through the solutions before and during the experiment.

**Spectrometer System.** Solutions were continuously recirculated from sample reservoir using a fast flow system with transfer speeds of ~1 m/s (pump pressure ~60 psi). Filtered solutions at high pressure passed through the irradiation tube in the variable magnetic field and then to the spinning 5 mm NMR sample tube in the probe of the Varian A56/60A NMR spectrometer before return to the reservoir at lower pressure. The flow system in the NMR probe was a modification of a similar system previously described.<sup>13</sup>

Solutions were irradiated with the 3 MeV electron beam from the Argonne Van de Graaff accelerator. The electron beam entered our irradiation magnet axially. During irradiation this magnetic field could be varied from ~30 to 6000 G.

## Results and Discussion

CIDNP in the products of pulse radiolysis of aqueous solutions of methanol, sodium acetate, iodomethane, ethylene glycol, and sodium chloroacetate were examined as a function of magnetic field from approximately 30 to 6000 G. The concentration of primary radicals was varied by changing reaction conditions. In N<sub>2</sub>O-saturated solutions OH radical predominates. In He-saturated solutions e<sub>aq</sub><sup>-</sup> and OH are both present in equal amounts together with some H radical; in He-saturated solutions at low pH e<sub>aq</sub><sup>-</sup> is largely converted to H radicals.<sup>4</sup> In several systems we have also investigated the effect of radical concentration by varying the electron beam. The *g* factors and hyperfine coupling constants of various radicals relevant to this study are summarized in Table I and the chemical shift assignments of the observed radical reaction products are summarized in Table II.

**Methanol System.** CIDNP in products from pulse radiolysis of aqueous methanol was most extensively studied. The magnetic field dependence of CIDNP in this system illustrates the

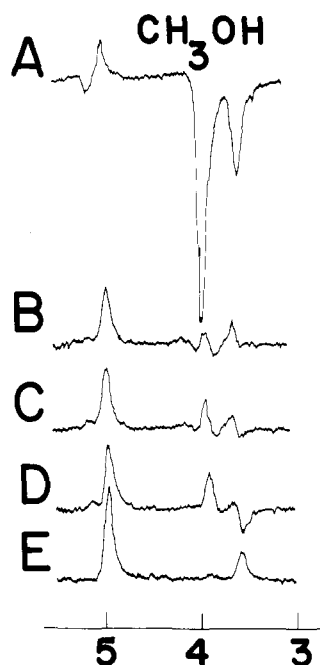


Figure 1. Methanol-*d* (0.25 M) ( $N_2O$ , pH 5.4). Fields: A,  $\sim 30$  G; B, 2 kG; C, 4 kG; D, 6 kG; E, 6 kG (no beam).

Table I. *g* Factors and Hyperfine Coupling Constants

Radical	<i>g</i> factor	Coupling constants, G
$e_{aq}^-$ <sup>a</sup>	2.000 3	
D·(H·) <sup>b</sup>	2.002 23	77.45 (503.8)
CH <sub>3</sub> · <sup>b</sup>	2.002 5	-23.04
·CH <sub>2</sub> OH <sup>b,c</sup>	2.003 29	-17.56
·CH <sub>2</sub> COO <sup>-b</sup>	2.003 27	-21.2
·CHClCOO <sup>-b</sup>	2.006 47	-20.48
(·CHOH)CH <sub>2</sub> OH <sup>c</sup>	2.003 08	-9.9 ( $\alpha$ ), 17.5 ( $\beta$ )

<sup>a</sup> Reference 18. <sup>b</sup> Reference 19. <sup>c</sup> Reference 20.

analytical possibilities of CIDNP NMR study in pulse radiolysis. While at 4000 G only ethylene glycol can be observed in  $N_2O$ -saturated solutions,<sup>2</sup> examination of spectra in fields from  $\sim 30$ –6000 G provides numerous details on other reaction pathways of the ·CH<sub>2</sub>OH radical.

The  $N_2O$ -saturated solutions of methanol (CH<sub>3</sub>OD in D<sub>2</sub>O) show polarized products: ethylene glycol, methanol, and water. Figure 1 shows the observed polarized NMR spectra at various fields. At  $\sim 30$  G strong emission is observed in ethylene glycol, methanol, and water. The methanol emission is so intense that it inverts the solvent line of methanol entirely while the water line is only partly inverted. As the irradiation field is increased the polarization changes to the high-field situation. At 6000 G (Figure 1D) the water line is still partially reduced as compared to the "no beam" situation. Ethylene glycol is seen in enhanced absorption while the methanol line is in emission (actually it appears to be AE with excess E).

Methanol radiolysis in He-saturated solution is illustrated in Figure 2. Now the reaction system consists of OH,  $e_{aq}^-$ , and H radicals. Again at low field all radical products are in emission. The ethylene glycol line is somewhat less intense as compared to the methanol line but both show strong emission. The water line is strongly reduced (compare with "no beam" at low field in Figure 2A). In contrast to Figure 1 the intermediate field CIDNP of methanol does not change to absorption; rather methanol is always in E. However, some intensity change is seen. The most intense emission in methanol is seen at low field and at high field (6000 G in Figure 2F).

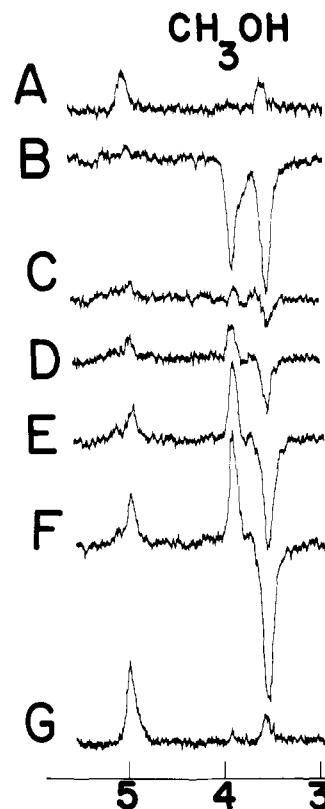


Figure 2. Methanol-*d* (0.1 M) (He, pH 5.4). Fields: A,  $\sim 30$  G (no beam); B,  $\sim 30$  G; C, 1 kG; D, 2 kG; E, 4 kG; F, 6 kG; G, 6 kG (no beam).

Table II. Chemical Shift Assignments

Compd	ppm (TMS)	Compd	ppm (TMS)
CH <sub>3</sub> OH	3.5	CH <sub>3</sub> I	2.3
CH <sub>3</sub> COO <sup>-</sup>	2.1	H <sub>2</sub> O	$\sim 5$
CH <sub>4</sub>	0.2	CH <sub>3</sub> CH <sub>2</sub> COO <sup>-</sup>	t 2.2, <sup>a</sup> q 2.4 <sup>b</sup>
CH <sub>3</sub> CH <sub>3</sub>	0.9	(CHClCOO <sup>-</sup> ) <sub>2</sub>	5.6
(CH <sub>2</sub> OH) <sub>2</sub>	3.7	(CHClCOO <sup>-</sup> )- CH <sub>2</sub> COO <sup>-</sup>	t 4.8, <sup>a</sup> d 3.2 <sup>c</sup>
(CH <sub>2</sub> COO <sup>-</sup> ) <sub>2</sub>	2.6	CH <sub>2</sub> ClCOO <sup>-</sup>	4.3
CH <sub>3</sub> CH <sub>2</sub> OH	t 2.15, <sup>a</sup> q 3.4 <sup>b</sup>		

<sup>a</sup> t = triplet. <sup>b</sup> q = quartet. <sup>c</sup> d = doublet.

Methanol radiolysis at pH 1.8 (He-saturated solution) is very interesting (Figure 3). Almost no ethylene glycol is seen except in intermediate irradiation fields. This was expected since we are dealing with the H and OH reaction system where most of the ·CH<sub>2</sub>OH radicals produced by OH react with H (actually D) to give back methanol. The methanol line is extremely intense E at low field, becomes AE at high field, and is mostly A in intermediate irradiation fields. Again the water line is always reduced (emission); this is most evident at low fields.

From this examination of CIDNP in aqueous methanol radiolysis several conclusions emerge. The principal radicals are ·CH<sub>2</sub>OH, H, and  $e_{aq}^-$ . Their encounters are responsible for polarization in ethylene glycol, methanol, and water. The polarization pathways are summarized in Scheme I.

The strong emission in methanol at high fields when  $e_{aq}^-$  is present strongly implies that the *g*-factor difference in a pair  $e_{aq}^-$ ·CH<sub>2</sub>OH is responsible. Similarly the  $e_{aq}^-$ ·H pair is probably responsible for the observed emission in water.

In the absence of  $e_{aq}^-$  in acidic solution methanol is observed

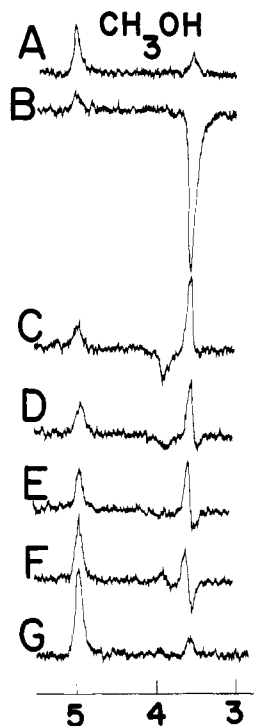
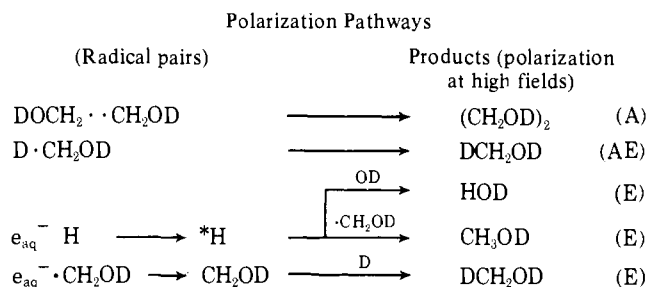
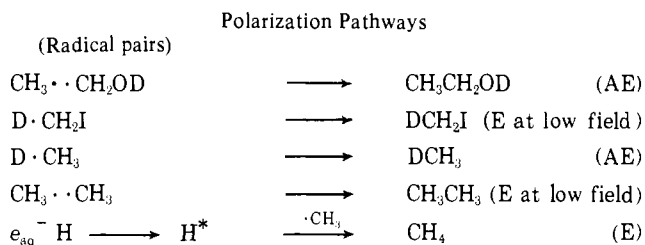


Figure 3. Methanol-*d* (0.1 M) (He, pH 1.8). Fields: A, ~30 G (no beam); B, ~30 G; C, 1 kG; D, 2 kG; E, 3 kG; F, 5 kG; G, 5 kG (no beam).

Scheme I. Methanol Systems [Radicals Present: OD,  $e_{aq}^-$ , D, H,  $\cdot\text{CH}_2\text{OD}$  (from OD +  $\text{CH}_3\text{OD}$ )]



Scheme II. Methanol-Iodomethane [Radicals Present: OD,  $e_{aq}^-$ , D, H,  $\cdot\text{CH}_2\text{OD}$ ,  $\cdot\text{CH}_3$  (from  $e_{aq}^- + \text{CH}_3\text{I}$ ),  $\cdot\text{CH}_2\text{I}$  (from OD +  $\text{CH}_3\text{I}$ )]



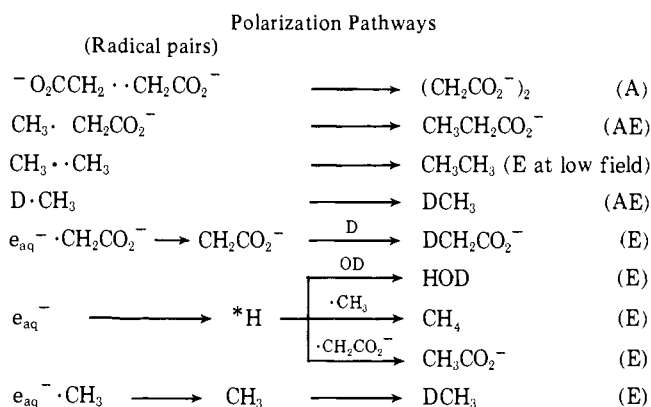
And pathways in Scheme I

AE. Clearly, this polarization arises from the  $\text{D} \cdot \text{CH}_2\text{OH}$  pair, since these two radicals have similar  $g$  factors.

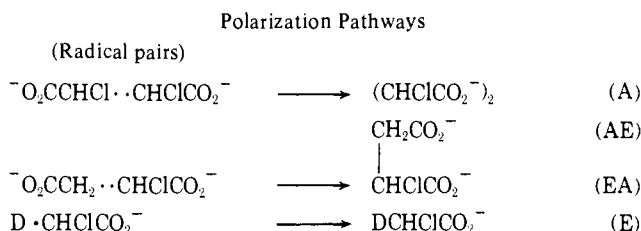
The observed polarization (A) of ethylene glycol at high fields and the magnetic field dependence of polarization suggest that other radicals with larger  $g$  factors are also present. Possibly oxygen centered radicals like  $\text{CH}_3\text{O} \cdot$  are involved.<sup>14</sup> This is under investigation.

That the H radical carries polarization is shown by the observed emission in water. In the case of emission in methanol this pathway could not be very important since in  $\text{D}_2\text{O}$  solution there is very little H. This is true in other pathways involving polarization carried by H (indicated by the asterisk) in Schemes I-IV.

Scheme III. Acetate Systems [Radicals Present: OD,  $e_{aq}^-$ , D, H,  $\cdot\text{CH}_2\text{CO}_2^-$ , and  $\cdot\text{CH}_3$  (from OD +  $\text{CH}_3\text{CO}_2^-$ )]



Scheme IV. Acetate-Chloroacetate [Radicals Present: OD,  $e_{aq}^-$ , D, H,  $\cdot\text{CH}_2\text{CO}_2^-$ ,  $\cdot\text{CH}_3$ ,  $\cdot\text{CHClCO}_2^-$  (from OD +  $\text{CH}_2\text{ClCO}_2^-$ )]



And pathways in Scheme III

While probably most of  $e_{aq}^-$  reacts with H (D) to give  $\text{H}_2$  some  $e_{aq}^-$  undergoes nonreactive encounters with H. As is the case with all reactions exhibiting CIDNP only a small fraction of the total reaction may proceed through the latter pathway. However, these nonreactive encounters with  $e_{aq}^-$  appear to be responsible for emission observed in the products from many other radicals as will be illustrated.

**Methanol-Iodomethane Systems.** The aqueous solution of methanol and iodomethane presents the opportunity to study reaction of radicals that are produced by both primary radicals. OH reacts predominately with methanol to give  $\cdot\text{CH}_2\text{OH}$  radical while  $\cdot\text{CH}_3$  radical is produced by  $e_{aq}^-$  reaction with iodomethane.

In  $\text{N}_2\text{O}$ -saturated solution (Figure 4) the radicals  $\cdot\text{CH}_2\text{OH}$ ,  $\cdot\text{CH}_3$ , and H give rise to the following polarized products: ethanol, methanol, methane, ethane, ethylene glycol, and water. Iodomethane can also be seen in emission at low fields. All products exhibit strong polarization at low field with ethanol exhibiting typical near-zero-field multiplet intensities. Increase of the irradiation field reduces the CIDNP intensities and at high fields polarizations of iodomethane and methane are harder to see and ethane polarization cannot be seen at all.

The He-saturated aqueous solution (Figure 5) shows polarization of the same products. However, emission in methane (actually  $\text{CH}_3\text{D}$ ) is more pronounced at high fields, methanol is now seen in E at high fields, and the relative amounts of polarized products are changed. The acidic solution of the methanol-iodomethane mixture is shown in Figure 6. The methane polarization is AE at high fields. Methanol is also AE at 6000 G.

Study of methanol-iodomethane solutions supports the assignment of the various polarization pathways in the methanol and methanol-acetate systems.<sup>2</sup> The most interesting feature is the polarization in methane ( $\text{CH}_3\text{D}$ ) and methanol, which depends on the reaction conditions. In He-saturated solution it is in emission due to  $e_{aq}^-$  participation in the polarization pathway, as observed before for  $\cdot\text{CH}_2\text{OH}$ . Acidic solutions yield  $\text{CH}_3\text{D}$  in AE from the  $\text{D} \cdot \text{CH}_3$  pair. Polarization

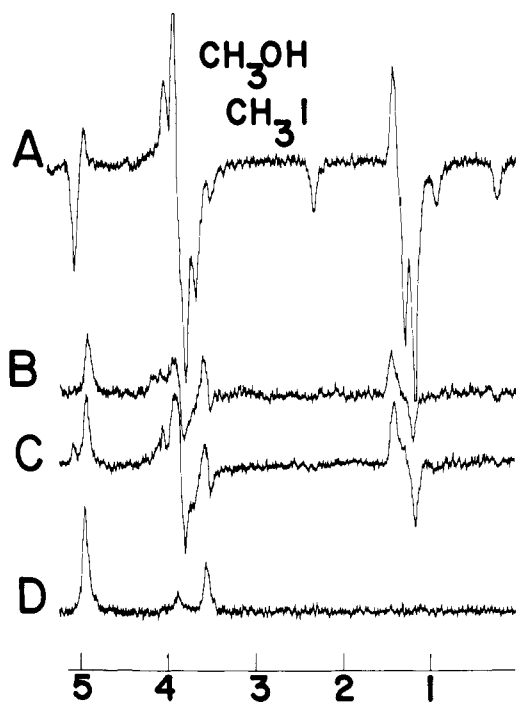


Figure 4. Methanol-iodomethane ( $\text{N}_2\text{O}$ , pH 5.5). Fields: A,  $\sim 30$  G; B, 2 kG; C, 6 kG; D, 6 kG (no beam).

of methanol is analogous. The emission in ethane can be observed only at low fields which is in agreement with the  $\text{S-T}_{-1}$  polarization pathway.<sup>15</sup>

At low fields in both  $\text{N}_2\text{O}$ - and He-saturated solutions iodomethane is also observed. This product probably arises from the pair  $\text{D}\cdot\text{CH}_2\text{I}$ , where  $\cdot\text{CH}_2\text{I}$  results from OH abstraction.

**Ethylene Glycol.** We have examined  $\text{N}_2\text{O}$ - and He-saturated solutions of ethylene glycol. In both cases the radical from ethylene glycol is produced by hydrogen abstraction by OH. It predominantly reacts with itself in the OH reaction system or with H when it is available.

These results are consistent with our time-resolved EPR study of the radical from ethylene glycol which indicated that the radical disappearance occurs through reaction of the ethylene glycol radical with itself (or a radical with similar  $g$  factor) in  $\text{N}_2\text{O}$ -saturated solutions.<sup>6</sup>

CIDNP is most pronounced at low fields, indicating that  $\text{S-T}_{-1}$  mixing is operative.

In He-saturated solution the principal polarized product is ethylene glycol itself. The strong emission probably originates in the  $e_{\text{aq}}^- \cdot \text{CH}(\text{OH})\text{CH}_2\text{OH}$  radical pair because of the large  $g$ -factor difference. Very little coupling product can be seen. Water is also in emission, which arises via the  $e_{\text{aq}}^-$  polarization outlined before.

**Sodium Acetate.** Reactions of the  $\cdot\text{CH}_2\text{COO}^-$  radical produced in the radiolysis of acetate have been studied by time-resolved EPR study spectroscopy<sup>5,6</sup> and by NMR CIDNP.<sup>2</sup> The time-resolved EPR study of the radical from acetate indicates that the principal radical reactions are among these radicals themselves or with radicals having similar  $g$  factors.

Several polarized products are observed in the CIDNP study of pulse radiolysis of acetate solutions (Figures 7–10). Succinate appears in enhanced absorption, propionate has two polarized AE multiplets (quartet at 2.4 ppm and triplet at 1.2 ppm), and methane can be seen at 0.2 ppm and ethane at 0.8 ppm. In more dilute solutions of acetate, acetate itself and  $\text{H}_2\text{O}$  show polarization. Figure 7 illustrates the CIDNP observed in  $\text{N}_2\text{O}$ -saturated solutions of acetate (acetate is at 2.1 ppm).

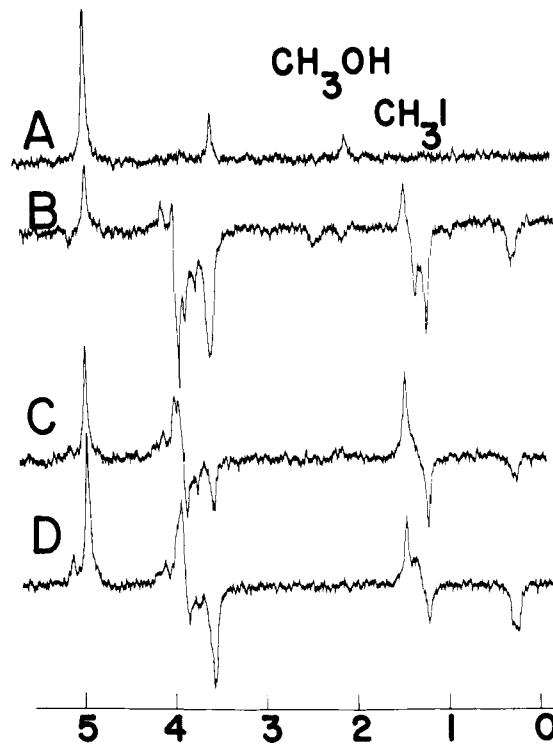


Figure 5. Methanol-iodomethane (He, pH 5.3). Fields: A,  $\sim 30$  G (no beam); B,  $\sim 30$  G; C, 2 kG; D, 6 kG.



Figure 6. Methanol-iodomethane (He, pH 1.8). Fields: A,  $\sim 30$  G; B, 2 kG; C, 4 kG; D, 6 kG; E, 6 kG (no beam).

When irradiation was carried out in very low fields, propionate shows typical near-zero-field multiplet effects and methane is in emission. At high fields propionate shows AE multiplets, methane is in enhanced absorption, and ethane cannot be seen.

He-saturated solutions of acetate were examined (Figure 8) and very similar polarization is observed in all products

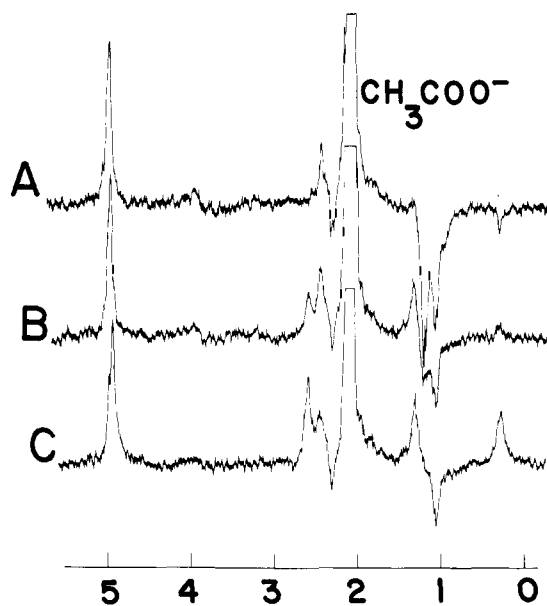


Figure 7. Sodium acetate (2.5 M) ( $\text{N}_2\text{O}$ , pH 7.6). Fields: A,  $\sim 30$  G; B, 1 kG; C, 6 kG.

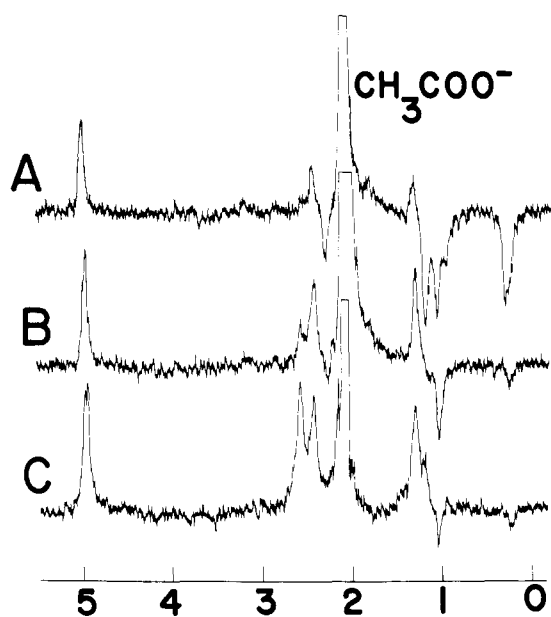


Figure 8. Sodium acetate (2.5 M) (He, pH 7.5). Fields: A,  $\sim 30$  G; B, 1 kG; C, 6 kG.

except that of methane which is now in emission at high fields. Again ethane can be seen only at very low irradiation field.

Lower concentrations of acetate were also examined. Figure 9 illustrates the  $\text{N}_2\text{O}$ -saturated solution of sodium acetate (0.4 M). At low fields succinate, acetate, and water are seen in emission. Very little propionate can be seen. In high field succinate is in enhanced absorption, acetate is in emission, and methane is in enhanced absorption.

The He-saturated solution of sodium acetate at this lower concentration is shown in Figure 10. Polarization of all products is the same except that of methane, which is in emission at both low and high fields. The intensities of succinate and acetate polarization at high fields are quite remarkable.

Higher concentrations of acetate yield more methane. As one can conclude from the chloroacetate experiments, methane occurs from OH reaction with acetate and *not* from the acetate radical itself. Scheme II summarizes various polarization pathways. Propionate polarization occurs in the  $\text{CH}_3\cdot$

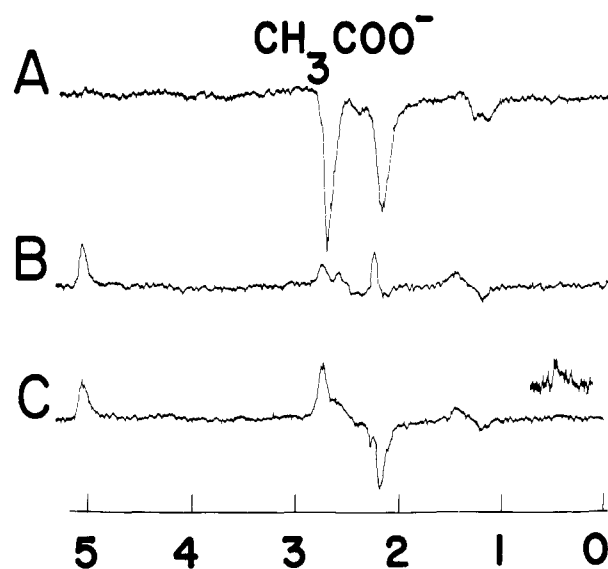


Figure 9. Sodium acetate (0.4 M) ( $\text{N}_2\text{O}$ , pH 6.9). Fields: A,  $\sim 30$  G; B, 2 kG; C, 6 kG (inset: gain  $\times 2.5$ ).

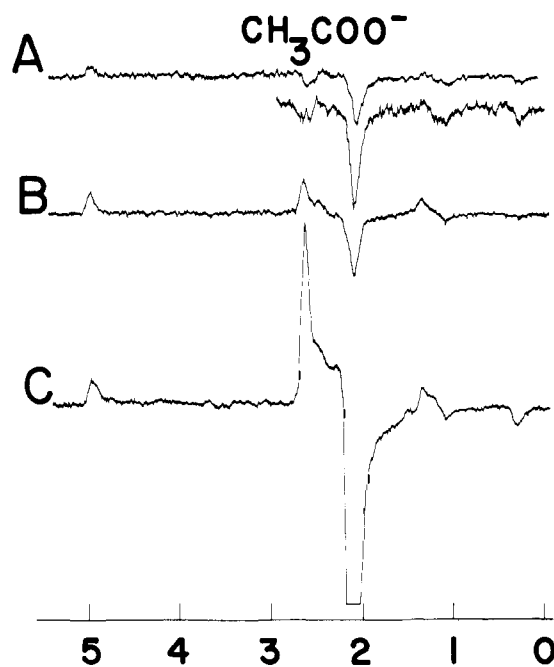


Figure 10. Sodium acetate (0.4 M) (He, pH 6.9). Fields: A,  $\sim 30$  G (inset: gain doubled); B, 2 kG; C, 6 kG.

$\text{CH}_2\text{CO}_2^-$  pair and is AE as expected. Acetate and methane owe their polarization to the presence of hydrated electron as described before. Thus the polarization of methane ( $\text{CH}_3\text{D}$ ) in high fields is an apt illustration of the various reaction pathways followed as the reaction conditions are varied. In the OH reaction system ( $\text{N}_2\text{O}$ -saturated solution) methane can be seen in absorption since in this system it is the radical with the smallest  $g$  factor. When  $e_{\text{aq}}^-$  is present methane is observed in emission by the already discussed polarization pathway.

**Chloroacetate-Acetate System.** Sodium chloroacetate yields  $\cdot\text{CH}_2\text{COO}^-$  radical by dissociative electron capture and  $\cdot\text{CHClCOO}^-$  radical by OH abstraction. Solutions of chloroacetate alone and as a mixture with sodium acetate were examined.

Figure 11 illustrates the CIDNP in He-saturated aqueous chloroacetate solution. Numerous products can be seen. At 5.5 ppm a combination product of two chloroacetate radicals

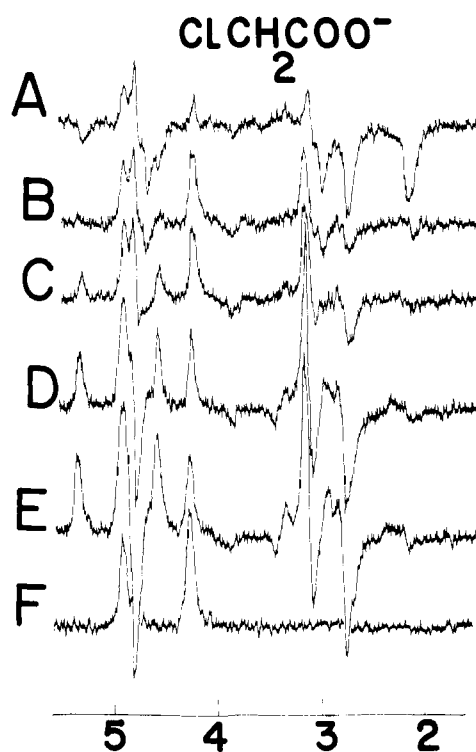


Figure 11. Sodium chloroacetate (0.4 M) (He, pH 4.4). Fields: A,  $\sim 30$  G; B, 1 kG; C, 2 kG; D, 4 kG; E, 6 kG; F, 6 kG (no beam).

$(\text{ClCHCOO}^-)_2$  is noted. A cross combination product  $(\text{CHClCOO}^-)\text{CH}_2\text{COO}^-$  is assigned to the 4.7 ppm triplet and 3 ppm doublet. Acetate can be seen in emission at 2.1 ppm and succinate is also in emission at 2.7 ppm. Chloroacetate itself shows some reduction in intensity especially at low field (Figure 11A at 4.2 ppm). There are several other polarized products whose identities could not be established, e.g., absorptions near 3.3 ppm.

When chloroacetate solutions were acidified, the spectra in Figure 12 were obtained. There is less dichloro product  $(\text{CHClCOO}^-)_2$ . Acetate is AE at 2.1 ppm at high field. The cross product  $(\text{CHClCOO}^-)\text{CH}_2\text{COO}^-$  is very strongly polarized.

Mixtures of excess sodium acetate and chloroacetate (Figure 13) in He-saturated solution yield methane and propionate. No dichlorosuccinate can be seen and the cross product is produced in smaller quantities.

The study of this system further substantiates our previous assignment of products and polarization pathways. Chloroacetate alone produces products from two radicals  $\cdot\text{CH}_2\text{COO}^-$  and  $\cdot\text{CHClCOO}^-$ . The coupling product of these two radicals shows multiplet polarization with substantial  $g$ -factor contribution. No methane can be seen except when acetate is present. This clearly illustrates that methyl radical is produced by OH reaction with acetate. In He-saturated solution acetate can be seen in AE; otherwise it is E at high fields. Polarization pathways are summarized in Scheme IV.

### Conclusions

The study of pulse radiolysis by NMR CIDNP techniques can yield numerous details of radical reaction mechanisms. The variable field CIDNP study together with the variation of reaction conditions allows assignment of almost all reaction products in the systems studied. The observation of polarization in all starting materials illustrates the advantages of NMR CIDNP study over more tedious product analysis. Furthermore, in addition to enabling us to detect and assign various products of radiolysis, details of some reaction pathways that

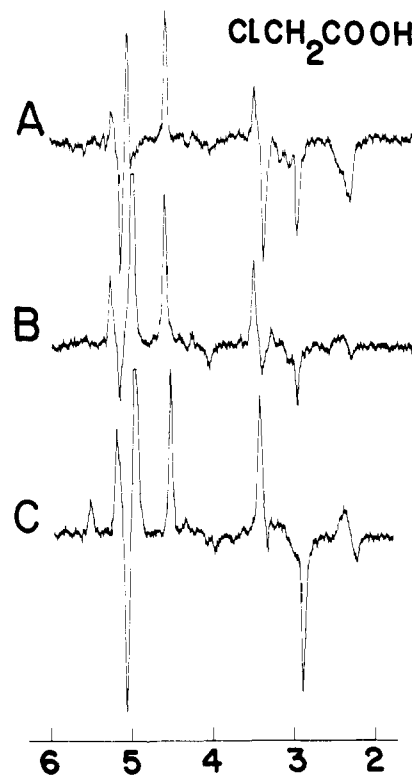


Figure 12. Sodium chloroacetate (0.4 M) (He, pH 1.8). Fields: A,  $\sim 30$  G; B, 2 kG; C, 6 kG.

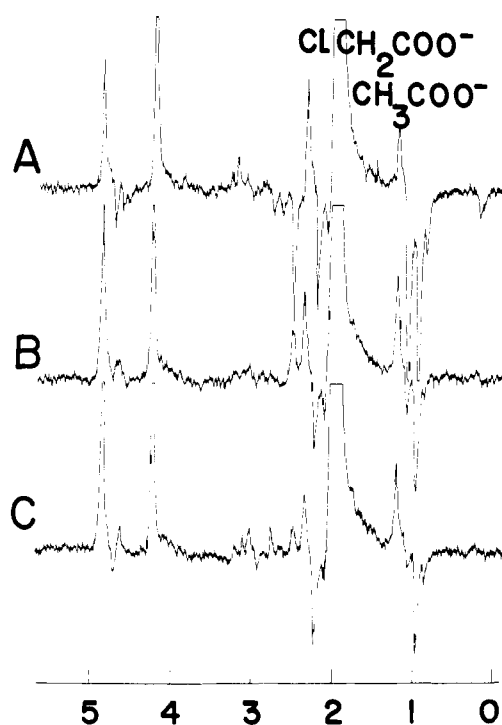


Figure 13. Sodium acetate (2.5 M)/sodium chloroacetate (0.4 M) (He, pH 6.9). Fields: A,  $\sim 30$  G; B, 2 kG; C, 6 kG.

yield these products can be defined. As merely one example, the strong emissions in methane, methanol, and other products which arise from the reaction of  $e_{\text{aq}}^-$  with  $\cdot\text{CH}_3$ ,  $\cdot\text{CH}_2\text{OH}$ , or other appropriate radicals illustrate the importance of  $e_{\text{aq}}^-$  in the polarization pathway.<sup>16</sup> It is particularly revealing that the primary radicals of pulse radiolysis ( $e_{\text{aq}}^-$  and H) play such an important role in the CIDNP of products.

Because higher radical concentrations were used in these studies, radical lifetimes were quite short ( $1 \mu\text{s}$  or less). How-

ever, it is believed that polarization needs several tens of a nanosecond to develop. Thus it may be possible to use CIDNP NMR to study the inhomogeneous reactions of radiation chemistry ("spurts", etc.).

Despite their differences, the common feature of both magnetic polarization methods, CIDEP and CIDNP, is that each reveals in its own fashion the memory of radical interactions in solution.<sup>17</sup> As a result, in addition to the many facets of solution microdynamics which are revealed, both techniques can be superb tools for the study of radical reaction mechanisms in solution. This is especially true in radiation chemistry where it may be possible to show that the polarization-producing pathways can quantitatively reflect the bulk of radical reactions in solution.

**Acknowledgments.** This work could not have been possible without the expert help of K. W. Johnson in all aspects of instrument design. We wish to thank the operators of the Argonne Van de Graaff, R. H. Lowers and A. Youngs, for their efforts.

### References and Notes

- (1) Work performed under the auspices of the U.S. Energy Research and Development Administration.
- (2) Paper I: A. D. Trifunac, K. W. Johnson, and R. H. Lowers, *J. Am. Chem. Soc.*, **98**, 6067 (1976).

- (3) Summer faculty research participant at ANL.
- (4) General references. M. S. Matheson and L. M. Dorfman, "Pulse Radiolysis", MIT Press, Cambridge, Mass., 1969. J. W. T. Spinks and R. J. Woods, "An Introduction to Radiation Chemistry", 2nd ed, Wiley-Interscience, New York, N.Y., 1976.
- (5) R. W. Fessenden, *J. Chem. Phys.*, **58**, 2489 (1973).
- (6) A. D. Trifunac and M. C. Thurnauer, *J. Chem. Phys.*, **62**, 4889 (1975).
- (7) A. D. Trifunac, K. W. Johnson, B. E. Clifft, and R. H. Lowers, *Chem. Phys. Lett.*, **35**, 566 (1975).
- (8) A. R. Lepley and G. L. Closs, Ed., "Chemically Induced Magnetic Polarization", Wiley-Interscience, New York, N.Y., 1973.
- (9) G. L. Closs and A. D. Trifunac, *J. Am. Chem. Soc.*, **92**, 2183 (1970).
- (10) R. Kaptein, *Chem. Commun.*, 732 (1971); A. D. Trifunac, Ph.D. Thesis, Chicago, Ill., 1971.
- (11) The exchange coupling ( $J$ ) is usually quite small and thus considered unimportant in CIDNP.<sup>12</sup> However, the observation of CIDEP in these systems indicates that  $J$  is not zero.
- (12) G. L. Closs, *Adv. Magn. Reson.*, **7**, 157 (1974).
- (13) R. G. Lawler and M. Halfon, *Rev. Sci. Instrum.*, **45**, 84 (1974).
- (14) J. A. Wargon and F. Williams, *J. Am. Chem. Soc.*, **94**, 7917 (1972).
- (15) J. A. Den Hollander, Ph.D. Thesis, Leiden, 1976; *Chem. Phys.*, **10**, 167 (1975).
- (16) The observation of polarization in the products of radicals that undergo a nonreactive encounter with  $e_{aq}^-$ , before they encounter H radical to give products, illustrates the carry over of polarization. This has been discussed in some detail by Den Hollander.<sup>15</sup>
- (17) We are investigating whether there is any transfer of polarization between the electron and nuclear spin systems. One of the referees has raised this point concerning the possible cross-relaxation polarization transfer between CIDEP in radicals and CIDNP in their products.
- (18) E. C. Avery, J. R. Remko, and B. Smaller, *J. Chem. Phys.*, **49**, 951 (1968); F. P. Sargent and E. M. Gardy, *Chem. Phys. Lett.*, **39**, 188 (1976).
- (19) R. W. Fessenden and R. H. Schuler, *J. Chem. Phys.*, **39**, 2147 (1963).
- (20) R. Livingston and H. Zeldes, *J. Chem. Phys.*, **44**, 1245 (1966).

## Photoelectron Spectra of Solid Inorganic and Organometallic Compounds Using Synchrotron Radiation. Valence Band Spectra and Ligand Field Broadening of Core d Levels

G. M. Bancroft,\*<sup>1a</sup> T. K. Sham,<sup>1a</sup> D. E. Eastman,<sup>1b</sup> and W. Gudat<sup>1b</sup>

Contribution from the Chemistry Department, University of Western Ontario, London N6A 5B7, Canada, and the IBM Thomas J. Watson Research Centre, Yorktown Heights, New York 10598. Received September 3, 1976

**Abstract:** Using synchrotron radiation from the Wisconsin storage ring as the photon source, we have obtained valence band and outermost d core level photoelectron spectra of a number of solid Sn, In, Sb, and Pb organometallic and inorganic compounds containing phenyl (Ph), methyl (Me), chloride, and acetylacetonates (AcAc, BzAc, BzBz) as ligands. With a total instrumental resolution of 0.3 eV at 57 eV photon energies, we have obtained d core line widths in the low 0.7 eV region, within 0.15 eV of the corresponding metal line widths. Correlations of the Sn 4d line widths and chemical shifts with previously obtained 3d widths and shifts show that we have minimized experimental difficulties such as charging and decomposition. The resolution in the valence band region is good enough to detect and assign a large number of the valence band peaks. For example, eight valence band peaks can be resolved in the Ph<sub>4</sub>Sn spectrum, and these peaks can be assigned readily to the benzene molecular orbitals and the Sn-C bonding orbitals. The routinely variable photon energy is sometimes useful for assigning peaks in these spectra. The broadening of the Sn 4d peaks is attributed to an unresolved ligand field splitting. In particular, the broadening is due to the asymmetry or electric field gradient  $C_2^0$  term in the crystal field expansion. From the known nuclear field gradients, the magnitude of the  $C_2^0$  term ( $-0.036 \pm 0.006$  eV) in the Me<sub>2</sub>Sn compounds is shown to be consistent with the  $|C_2^0|$  values observed previously for Me<sub>2</sub>Cd (0.026 eV), XeF<sub>2</sub> (0.042 eV), and XeF<sub>4</sub> (0.043 eV). These results show that the electric field gradient splitting has to be considered as an important broadening mechanism (and splitting mechanism at very high resolutions) in photoelectron and adsorption studies. The 4d and 5d spin-orbit splittings do not vary with the chemical environment. However, the ratio of the  $d_{5/2}:d_{3/2}$  intensities appears to be sensitive to the chemical environment and varies considerably from the theoretical 1.5:1 ratio expected in an independent particle picture.

Photoelectron spectroscopy has been divided into two distinct areas because of the availability of simple intense light sources. If the photon energy is in the vacuum ultraviolet (VUV) range [for example, He(I) (21.2 eV) or He(II) (40.8 eV)], the technique is often called ultraviolet photoelectron spectroscopy (UPS).<sup>2a</sup> If the photon energy is in the x-ray range [for example, Mg K $\alpha$  (1253 eV) or Al K $\alpha$  (1486 eV)],

the technique is called x-ray photoelectron spectroscopy (XPS or ESCA).<sup>2b</sup> The former technique has been used predominantly to study valence levels of gases at high instrumental resolution ( $\leq 20$  meV) and solids at lower resolution ( $\leq 0.3$  eV), while the latter technique is used normally to study core levels at comparatively low resolution ( $\geq 0.6$  eV). In the x-ray case, the large line widths usually observed arise mainly from the